Quantum Wave Function Simulation of the Resonance Fluorescence Spectrum from One-Dimensional Optical Molasses

P. Marte,[1] R. Dum,[1] R. Taïeb,[1] P. D. Lett,[2] and P. Zoller[1]
[1] *Joint Institute for Laboratory Astrophysics, University of Colorado, Boulder, Colorado 80309-0440*
[2] *National Institute of Standards and Technology, Gaithersburg, Maryland 20899*
(Received 11 March 1993)

Using recently developed quantum wave function techniques, we have performed a simulation of ^{85}Rb atoms in a one-dimensional optical molasses, formed from counterpropagating laser beams with orthogonal linear polarizations. Both internal and external degrees of freedom are treated quantum mechanically in one dimension and the spectrum of resonance fluorescence is calculated and compared to recent experiments. Excellent agreement is obtained for the spectrum and additional insight is gained into the experimental evidence for quantized motion in the optical potentials.

PACS numbers: 32.80.Pj, 42.50.Ar

Two recent experiments [1,2] have reported evidence of quantized atomic motion in one-dimensional (1D) optical molasses. In the experiment of Jessen *et al.* [2] well-resolved "motional" sidebands due to spontaneous Raman transitions between vibrational levels in the optical potentials were observed in the fluorescence spectrum of ^{85}Rb atoms. A similar experiment has reported the observation of stimulated Raman transitions in an absorption spectrum of Cs [1]. Very recently, these quantized energy levels have been observed in 2D and 3D configurations [3,4].

The temperatures achieved in these experiments correspond to the accumulation of atoms in the few lowest vibrational energy levels of the optical potentials. Thus, a theoretical description of these phenomena should be based on a fully quantum mechanical treatment of atomic motion [5,6]. We report the results of such a quantum calculation for the spectrum of resonance fluorescence corresponding to the experiment of Jessen *et al.* [2]. The basis of the present work is a quantum Monte Carlo wave function simulation of the master equation for laser cooling [7,8]. This constitutes the first quantitative comparison between theory and experiment for the fluorescence spectrum of optical molasses, and one of the few quantitative comparisons of any kind in the field of laser cooling.

The basis of our theoretical discussion is the solution of the generalized optical Bloch equations for the atomic density matrix comprising both the internal and external (center-of-mass) degrees of freedom. The Rb atoms are driven on the $5S_{1/2}\ F_g = 3 \rightarrow 5P_{3/2}\ F_e = 4$ transition in a laser configuration consisting of two counterpropagating light beams with orthogonal linear polarizations [5]. This leads to a constant electric field amplitude, but a spatially varying polarization vector $\epsilon(z)$ with the laser propagation along the z axis. In this electric field the spatially varying Stark shifts of the $|F_g M_g\rangle$ ground states will form an alternating pattern of optical potentials where minima will occur for the states $|F_g M_g = \pm 3\rangle$ at positions with pure $\sigma^{\pm}$ light. Spontaneous emission will cause transitions between these potentials. For red laser detunings, $\Delta = \omega - \omega_{eg} < 0$, this gives rise to polarization gradient cooling. In the semiclassical picture this cooling mechanism is explained in terms of Sisyphus cooling [9]: one considers an atom moving on one of the potential curves with transitions to the other potentials occurring preferentially from higher points on the original potential to lower points on the subsequent one. On the average the atomic motion is damped. For small saturation parameters $s_0 = \Omega^2/2/(\Delta^2 + \Gamma^2/4) \ll 1$ the excited states can be eliminated. Here Ω is the maximum Rabi frequency on the $M_g = 3$ to $M_e = 4$ transition , and Γ is the spontaneous emission rate.

The corresponding master equation for the density matrix ρ of the ground state manifold and 1D motion in the z direction is [5,6] ($\hbar = 1$)

$$\frac{d}{dt}\rho = -i[H_{\rm eff}(\hat{z})\rho - \rho H_{\rm eff}^{\dagger}(\hat{z})] + \gamma_0 \sum_{\sigma} \int_{-k}^{+k} dk'_z\, N_{\sigma}(k'_z) B_{\sigma}(\hat{z}) e^{-ik'_z\hat{z}} \rho B_{\sigma}^{\dagger}(\hat{z}) e^{ik'_z\hat{z}}. \quad (1)$$

Here $k = 2\pi/\lambda$ is the wave vector, $N_{\sigma}(k'_z)$ is the angular distribution of spontaneous photons with polarization $\sigma = 0, \pm 1$, and $\gamma_0 = s_0\Gamma/2$ is the photon scattering rate. The first two terms in (1) involve the non-Hermitian atomic Hamiltonian

$$H_{\rm eff}(\hat{z}) = \frac{\hat{p}^2}{2M} - \left(U_0 + i\frac{1}{2}\gamma_0\right) \sum_{\sigma} B_{\sigma}^{\dagger}(\hat{z}) B_{\sigma}(\hat{z}), \quad (2)$$

describing the motion of the atomic wave packet with kinetic energy $\hat{p}^2/2M$ in a multicomponent optical potential with depths determined by $U_0 = s_0|\Delta|/2$. The real part of the potential in (2) gives rise to quantized energy levels (band structure), while the imaginary part describes a loss rate due to optical pumping. The operators $B_{\sigma}(z)$ correspond to Raman transitions between the ground state levels by absorption of a laser photon and subsequent emission of a spontaneous photon with polarization σ; see Ref. [6].

The spectrum of resonance fluorescence, emitted along the z axis, with frequency ω' and polarization σ, is given by the Fourier transform of the station-

0031-9007/93/71(9)/1335(4)$06.00

ary atomic dipole correlation function $c_\sigma(t-t_0) = \langle B_\sigma^\dagger(t) e^{ik_z'\hat{z}(t)} B_\sigma(t_0) e^{-ik_z'\hat{z}(t_0)}\rangle$ [6]. According to the quantum regression theorem [8] we have

$$c_\sigma(t-t_0) = \mathrm{Tr}_A\{B_\sigma^\dagger(\hat{z})\, e^{ik_z\hat{z}}\, \rho^{(1)}(t)\} \quad (t \geq t_0)\,, \quad (3)$$

where the first order perturbed density operator $\rho^{(1)}(t)$ obeys the same master equation as the density matrix but with a different initial condition

$$\rho^{(1)}(t_0) = B_\sigma(\hat{z})\, e^{-ik_z'\hat{z}}\rho(t_0)\,. \quad (4)$$

A direct solution of the master equation (1) to calculate the autocorrelation function (3) is impractical due to the large dimensionality of the density matrix equation which involves N^2 elements [$N = N_{\mathrm{ex}} \times N_{\mathrm{int}}$, where N_{int} is the number of internal, and N_{ex} the number of (discretized) external degrees of freedom]. A *simulation* of the quantum master equation in terms of *wave functions* can replace the *solution* of the master equation for the *density matrix* [7,8]. An important feature of the wave function approach is that one only has to deal with a wave function of dimension N, as opposed to working with the density matrix which has N^2 elements. In our case of ^{85}Rb we have $N = 448$ on a Fourier grid with 64 points corresponding to momenta up to $\pm 32\hbar k$ [6]; 10 000 wave function realizations are needed for convergence. This algorithm allowed a gain of about a factor of 50 in computing time over a density matrix calculation. We emphasize that our Monte Carlo method based on time-dependent Bloch functions treats the atomic momentum as a continuous variable; i.e., we do *not* assume a discretization of atomic momenta [6], an assumption which is inherent in any master equation treatment. Furthermore, parallelizing the simulation algorithm allows the calculations to be performed on a distributed system of networked computers as we have done, with a corresponding gain in computational power. In the approach of Refs. [6,8], the simulation consists of propagation of an atomic wave function $|\Psi(t)\rangle$ with the non-Hermitian (damped) atomic Hamiltonian (2) interrupted at random times by wave function collapses ("quantum jumps")

$$|\Psi(t)\rangle \rightarrow e^{ik_z'\hat{z}} B_\sigma(\hat{z})|\Psi(t)\rangle, \quad (5)$$

and subsequent wave function renormalization. The Schrödinger equation for $|\Psi(t)\rangle$ describes the time evolution of the atomic wave packet in the periodic optical potential, and its coupling to the laser driven internal atomic dynamics. The times of the "quantum jumps" are selected according to the delay function

$$P(t, k_z', \sigma) = N_\sigma(k_z')\, 2\gamma_0 \,\|\, B_\sigma(\hat{z})|\Psi(t)\rangle \,\|^2\,, \quad (6)$$

which gives the probability for emitting a spontaneous photon at time t, with momentum k_z' along the z axis and polarization σ. The "quantum jump" (5) corresponds to an optical pumping process between the atomic ground states, including the associated momentum transfer to the atom. Averaging over these wave function realizations gives the density matrix $\rho(t) = \langle |\Psi(t)\rangle\langle\Psi(t)| / \|\Psi(t)\|^2\rangle$. The dipole correlation function (3) can be simulated following the approach developed in Refs. [6,8]. The perturbed density matrix $\rho^{(1)}(t)$ in Eq. (3) can be interpreted as a first order response to a "delta kick" at time $t = t_0$, represented by the initial condition (4). A simulation is obtained by introducing a "perturbed" wave function $|\beta_{t_0}(t)\rangle$ which obeys the Schrödinger equation for $|\Psi(t)\rangle$ but now with initial condition [compare Eq. (4)]

$$|\beta_{t_0}(t_0)\rangle = e^{-ik_z'\hat{z}} B_\sigma(\hat{z})|\Psi(t_0)\rangle, \quad (7)$$

and quantum jumps of $|\beta_{t_0}(t)\rangle$ dictated by the wave function $|\Psi(t)\rangle$ according to the delay function (6). The dipole correlation function is

$$c_\sigma(t-t_0) = \langle\langle \Psi(t)|B_\sigma^\dagger(\hat{z}) e^{ik_z'\hat{z}}|\beta_{t_0}(t)\rangle / \|\Psi(t)\|^2\rangle\,, \quad (8)$$

where the bold angular brackets indicate averaging over both quantum jumps and initial times t_0.

The periodicity of the atomic Hamiltonian (2) in space allows us to propagate the atomic wave packets as *time dependent Bloch functions* $\Psi(z,t) = 1/\sqrt{2\pi}\, e^{iqz} u_q(z,t)$ with $q \in (-k, k]$ a quasimomentum in the first Brillouin zone, and $u_q(z,t) = u_q(z+\lambda/2, t)$ a periodic multicomponent atomic wave function. The Hamiltonian evolution due to H_{eff} preserves q, while quantum jumps cause changes between families of Bloch functions, $q \rightarrow q'$. In practice, we propagate the Bloch function $u_q(z,t)$ on the unit cell of the lattice $z \in [0, \lambda)$ using a split-operator fast-Fourier transform method [6].

Figure 1 compares the resonance fluorescence spectrum for σ^+ polarized light obtained by simulation (solid line) with the experimental data of Jessen *et al.* [2] (crosses). The central line is scattering at the laser frequency while the first red and blue sidebands correspond to Raman transitions between adjacent vibrational bands in the optical potential. Following Ref. [2] the parameters were taken as $\Delta = -4\Gamma$, $\Lambda \equiv \Omega^2/\Gamma|\Delta| = 0.23$, which cor-

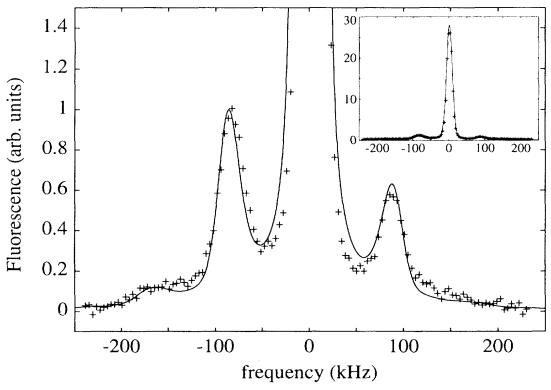

FIG. 1. Spectrum of resonance fluorescence as a function of the frequency ν. The parameters are $\Delta = -4\Gamma$, $\Lambda = 0.23$. The solid line is the theoretical spectrum convolved with a Lorentzian corresponding to a finite detector width of 3.8 kHz and a Gaussian with width 20 kHz (residual Doppler broadening). Crosses are the experimental result of Jessen *et al.* [2]. The inset shows the total spectrum.

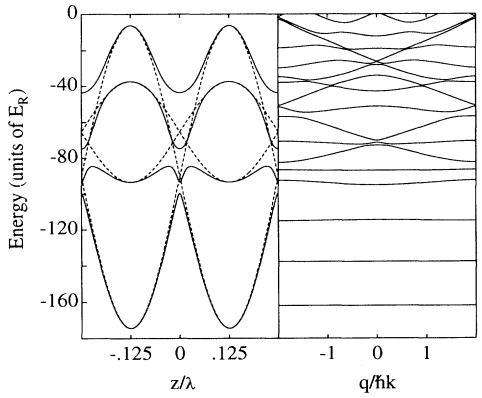

FIG. 2. In the left panel the optical potentials for odd M_F Zeeman sublevels of a ^{85}Rb atom ($F_g = 3 \rightarrow F_e = 4$) are plotted as a function of position z for the same parameters as Fig. 1. The solid (dashed) lines are the adiabatic (diabatic) potentials. In the right panel we have plotted the corresponding band structure as a function of the quasimomentum q.

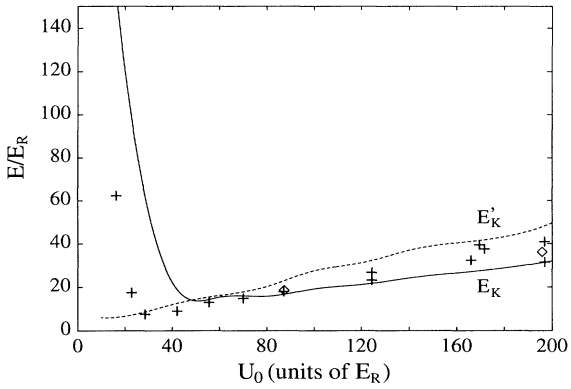

FIG. 3. Variation of the kinetic energy with the potential depth U_0. $E_k = \langle \hat{p}^2 \rangle / 2M$ is the expectation value of the kinetic energy and E'_k corresponds to the $1/\sqrt{e}$ width of the momentum distribution. The damping parameter γ_0 is fixed to $6E_R/\hbar$. The crosses are temperatures derived from the asymmetry of the experimental resonance fluorescence spectrum of Jessen *et al.* [2] *assuming* a Maxwell-Boltzmann distribution for the populations; the diamonds are the corresponding theoretical points derived from the Monte Carlo spectrum with the same analysis.

responds to a potential depth of $U_0 = 87E_R$ (with $E_R/\hbar = \hbar k^2/2M = 2\pi \times 3.85$ kHz the recoil energy). The theoretical spectrum was obtained by convolving the *ab initio* spectrum with a Lorentzian detector width of 3.8 kHz and a Gaussian with a width of 20 kHz [2]. The latter corresponds to residual Doppler broadening due to transverse motion of the atoms, detected because the experimental spectrum was measured at a small angle to the z axis.

The positions of the sidebands are determined by the Raman transition frequencies between the bands. Figure 2 shows the optical potentials and band structure for the parameters of Fig. 1. On the left-hand side of this figure the optical potentials (ac Stark shifts) for the laser coupled $M_g = \pm 3, \pm 1$ Zeeman sublevels are shown as a function of z/λ. The dashed lines correspond to the diagonal part of the multichannel potential. The solid lines are a set of adiabatic potentials obtained by diagonalization of the potential matrix. Because of optical pumping, most of the atomic population is accumulated in the $M_g = \pm 3$ states. In the right panel we plot the corresponding band structure as a function of the quasimomentum q in the first Brillouin zone $(-2\hbar k, 2\hbar k]$ [10].

The asymmetry of the red and blue sideband intensities reflects the populations of the vibrational levels, and thus the temperature of the atoms [2]. Agreement between experimental and theoretical asymmetries in Fig. 1 indicates that the wave function simulation predicts the correct spectrum but does not tell us if the asymmetry in the spectrum predicts the correct temperature. Figures 3 and 4 show the variation of the kinetic energy and the population of the lowest levels with the potential depth U_0, respectively. In Fig. 3, $E_k = \langle \hat{p}^2 \rangle / 2M$ is the expectation value of the kinetic energy, and E'_k corresponds to the $1/\sqrt{e}$ width of the momentum distribution. For a Maxwell-Boltzmann velocity distribution these two quantities would be equal; similarly, the ratio Π_n/Π_{n-1} in Fig. 4 would be a constant, and equal to the Boltzmann factor. In fact, we find a distribution which deviates from a Maxwell-Boltzmann distribution. As expected, the experimental data points with temperatures derived from the asymmetry of the sideband *assuming* a Maxwell-Boltzmann distribution lie between the two theoretical curves (crosses in Fig. 3); the diamonds are derived from the theoretical spectrum by a similar analysis. The kinetic energy shows a minimum near $U_0 = 60E_R$. This corresponds to a maximum population in the ground state of 42%. For the experimental parameters of Fig. 1 we find 35% of the total population (trapped and un-

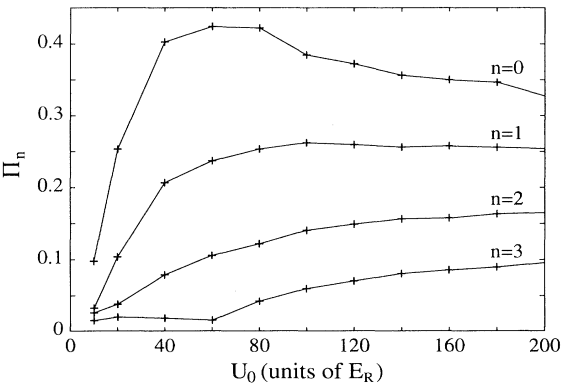

FIG. 4. Steady-state populations of the four first band levels for odd M_F Zeeman sublevels of a ^{85}Rb atom as a function of the potential depth U_0. The damping parameter γ_0 is fixed to $6E_R/\hbar$. The crosses correspond to the calculated points.

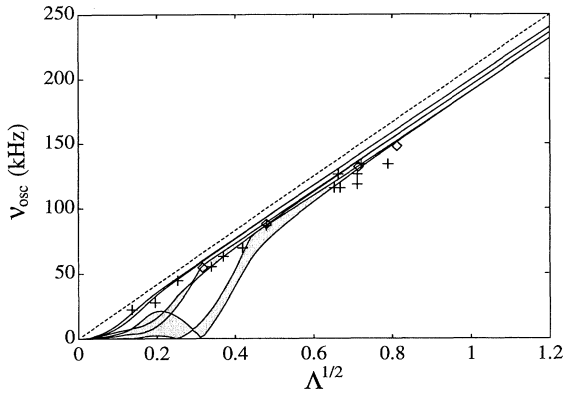

FIG. 5. Splitting frequency between sidebands and central peak as a function of $\Lambda^{1/2}$. The diamonds correspond to the theoretical position of the maximum of the sideband (after convolution) of the computed spectrum. The crosses correspond to the experimental data of Jessen *et al.* The dashed line is the oscillation frequency obtained with the harmonic approximation and the solid lines correspond to the computed maximum and minimum transition frequencies between the first four bands ($0 \rightarrow 1$, $1 \rightarrow 2$, $2 \rightarrow 3$).

trapped atoms) in the ground state.

Laser cooling accumulates atoms predominantly in the lowest vibrational states. This spatial localization of atoms—on a scale small compared with the laser wavelength—suppresses optical pumping transitions between different vibrational levels $n \neq n'$ (for the experiment in [2] we find localization of $\lambda/6$). This leads to a narrowing of the lines in the optical spectrum (Lamb-Dicke narrowing). For the parameters of Fig. 1 we have an optical pumping rate $\gamma_0 = 2\pi \times 84$ kHz. This should be compared with the width of 4.5 kHz for the central line, and 17 kHz for the sidebands.

A broadening mechanism is present for the sidebands, due to the anharmonicity of the optical potential. This leads to different transition frequencies for $n \rightarrow n \pm 1$ (by $\sim 1E_R/\hbar$). For the present parameters this anharmonicity is not resolved even in the unconvolved spectrum. The width of the sidebands in Fig. 1, however, is dominated by the experimental resolution. In Fig. 5 we compare the position of the motional sidebands obtained by the full quantum treatment with experimental data [2] and simplified theories. It turns out that only the full quantum calculation is able to produce the correct position, since it includes the anharmonic effect and shifts due to damping. Work in progress suggests that a full quantum treatment of the 2D case by this Monte Carlo wave function technique, including a calculation of the spectrum, is still a feasible problem. This again reveals the power of the present technique to handle extremely large problems, probably unapproachable by other methods.

The authors thank P. Jessen and the NIST laser cooling group for discussions. P.L. thanks J. Dalibard and K. Mølmer. This work is supported in part by the NSF (at JILA) and by the ONR (at NIST).

[1] P. Verkerk *et al.*, Phys. Rev. Lett. **68**, 3861 (1992).
[2] P.S. Jessen *et al.*, Phys. Rev. Lett. **69**, 49 (1992); P. S. Jessen, Ph.D. thesis, University of Aarhus, 1993.
[3] A. Hemmerich and T. W. Hänsch, Phys. Rev. Lett. **70**, 410 (1993).
[4] G. Grynberg *et al.*, Phys. Rev. Lett. **70**, 2249 (1993).
[5] Y. Castin and J. Dalibard, Europhys. Lett. **14**, 761 (1991); T. Bergeman (to be published).
[6] P. Marte *et al.*, Phys. Rev. A **47**, 1378 (1993).
[7] J. Dalibard *et al.*, Phys. Rev. Lett. **68**, 580 (1992); K. Mølmer *et al.*, J. Opt. Soc. Am. B **10**, 524 (1993); H. J. Carmichael (unpublished); N. Gisin and I.C. Percival, Phys. Lett. A **167**, 315 (1992).
[8] R. Dum *et al.*, Phys. Rev. A **45**, 4879 (1992); C. W. Gardiner *et al.*, *ibid.* **46**, 4363 (1992); R. Dum *et al.*, *ibid.* **46**, 4382 (1992).
[9] J. Dalibard and C. Cohen-Tannoudji, J. Opt. Soc. Am. B **6**, 2023 (1989); **2**, 1707 (1985).
[10] The periodic potential has the symmetry $z \rightarrow z + \lambda/4$, $M_g \rightarrow -M_g$, R. Taïeb *et al.*, Phys. Rev. A **47**, 4986 (1993).